Thermochemistry, Bond Energies, and Internal Rotor Potentials of Dimethyl Tetraoxide

Gabriel da Silva[†,‡] and Joseph W. Bozzelli*[,†]

Department of Chemistry and Environmental Science, New Jersey Institute of Technology, Newark, New Jersey 07102, and Department of Chemical and Biomolecular Engineering, University of Melbourne, Victoria 3010, Australia

Received: July 2, 2007; In Final Form: August 30, 2007

Thermochemical properties of dimethyl tetraoxide ($CH_3OOOOCH_3$), the dimer of the methylperoxy radical, are studied using ab initio and density functional theory methods. Methylperoxy radicals are known to be important intermediates in the tropospheric ozone cycle, and the self-reaction of methylperoxy radicals, which is thought to proceed via dimethyl tetraoxide, leads to significant chain radical termination in this process. Dimethyl tetraoxide has five internal rotors, three of them unique; the potential energy profiles are calculated for these rotors, as well as for those in the CH_3OO, CH_3OOO, and CH_3OOOO radicals. The dimethyl tetraoxide internal rotor profiles show barriers to rotation of 2−8 kcal mol^{-1}. Using B3LYP/6-31(d) geometries, frequencies, internal rotor potentials, and moments of inertia, we determine entropy and heat capacity values for dimethyl tetraoxide and its radicals. Isodesmic work reactions with the G3B3 and CBS-APNO methods are used; we calculate this enthalpy as −9.8 kcal mol^{-1}. Bond dissociation energies (BDEs) are calculated for all C−O and O−O bonds in dimethyl tetraoxide, again with the G3B3 and CBS-APNO theoretical methods, and we suggest the following BDEs: 46.0 kcal mol^{-1} for $CH_3-OOOOCH_3$, 20.0 kcal mol^{-1} for $CH_3O-OOOCH_3$, and 13.9 kcal mol^{-1} for $CH_3OO-OOCH_3$. From the BDE calculations and the isodesmic enthalpy of formation for dimethyl tetraoxide, we suggest enthalpies of 2.1, 5.8, and 1.4 kcal mol^{-1} for the CH_3OO, CH_3OOO, and CH_3OOOO radicals, respectively. We evaluate the suitability of 10 different density functional theory (DFT) methods for calculating thermochemical properties of dimethyl tetraoxide and its radicals with the 6-31G(d) and 6-311++G(3df,3pd) basis sets, using a variety of work reaction schemes. Overall, the best-performed DFT methods of those tested were TPSSh, BMK, and B1B95. Significant improvements in accuracy were made by moving from atomization to isodesmic work reactions, with most DFT methods yielding errors of less than 2 kcal mol^{-1} with the 6-311++G(3df,3pd) basis set for isodesmic calculations on the dimethyl tetraoxide enthalpy. These isodesmic calculations were basis set consistent, with a considerable reduction in error found by using the 6-311++G(3df,3pd) basis set over the 6-31G(d) basis set. This was not the case, however, for atomization and bond dissociation work reactions, where the two basis sets returned similar results. Improved group additivity terms for the O−O−O moiety (O/O_2 central atom group) are also determined.

Introduction

Peroxy radicals ($HOO^\bullet$ and $ROO^\bullet$) in the troposphere play an important role in the ozone cycle,[1] through the following reaction with NO

$$ROO^\bullet + NO \rightarrow RO^\bullet + NO_2 \quad (1)$$

NO_2 undergoes photodissociation to produce atomic oxygen and NO (eq 2), where atomic oxygen is known to react with O_2 to yield ozone (eq 3). Furthermore, NO will consume ozone in a reaction forming NO_2 and O_2 (eq 4). The combination of these reactions shows how the production of NO_2 (eq 4) and the consumption of NO (eq 1) leads to a net production of ozone

$$NO_2 + h\nu \rightarrow NO + O \quad (2)$$

$$O + O_2 + M \rightarrow O_3 + M \quad (3)$$

$$NO + O_3 \rightarrow NO_2 + O_2 \quad (4)$$

Peroxy radicals can be removed from the troposphere by their reactions with other peroxy radicals, with a negative impact on the rate of ozone production. Methyl peroxy radicals are one of the most atmospherically abundant organic peroxy radicals; self-reaction of the methyl peroxy radical has been well-studied experimentally,[2] and the process has been found to proceed by the overall reactions of eqs 5−7. A recent review of the experimental data on the methyl peroxy self-reaction suggested an overall rate constant of 3.5×10^{-13} cm^3 molecule^{-1} s^{-1} at 298 K,[3] although measured values for this rate constant span a range from 5.2×10^{-13} to 1.3×10^{-13} cm^3 molecule^{-1} s^{-1} at 298 K. The methyl peroxy self-reaction demonstrates a negative temperature dependence, although it is relatively insensitive to temperature, with an activation energy of only −0.73 kcal mol^{-1} between 200 and 400 K.[3] In the methyl peroxy self-reaction, only eqs 5 and 6 are of any real importance, with recommended branching ratios of 0.63 and 0.37, respectively.[3] The branching ratio for eq 7, however, is estimated to be <0.06.[3] We observe that eq 5 results in the chain termination of both peroxy radicals, while eq 6 results in the production of two methoxy radicals

$$2CH_3OO^\bullet \rightarrow CH_3OH + CH_2{=}O + O_2 \quad (5)$$

$$2CH_3OO^\bullet \rightarrow 2CH_3O^\bullet + O_2 \quad (6)$$

$$2CH_3OO^\bullet \rightarrow CH_3OOCH_3 + O_2 \quad (7)$$

While there are numerous kinetic studies on the methyl peroxy self-reaction,[2] relatively little is still known about the elementary

* Author to whom correspondence should be addressed. Phone: (973) 596-3459. Fax: (973) 596-3586. E-mail: bozzelli@njit.edu.
[†] New Jersey Institute of Technology.
[‡] University of Melbourne.

10.1021/jp075144f CCC: $37.00
Published on Web 11/06/2007

reaction processes involved in this reaction or the thermochemistry and intrinsic reaction kinetics of these elementary processes. Recent computational studies on this[4] and similar systems[5] have begun to elucidate aspects of these processes, and alkyl tetraoxides, such as dimethyl tetraoxide, have emerged as important intermediates. The experimental observation of a small negative activation energy suggests a chemically activated reaction mechanism, where the initial reaction step is a barrierless radical + radical association reaction.

The role that methyl peroxy radicals play in tropospheric chemistry has long been known, but it is a recent concern that these radicals may be important combustion intermediates, especially during low-temperature processes such as those in the cool-down zones of furnaces and in cool flame combustion systems. Methyl radicals will react with O_2, producing CH_3OO at lower temperatures, and products such as CH_3O and formaldehyde at elevated temperatures.[6] Recent studies within our research group on oxy-hydrocarbons important in low-temperature combustion processes, including formaldehyde,[7] the *n*-aldehydes,[8] and vinyl alcohol,[9] have identified several possible pathways for CH_3 formation. For example, vinyl alcohol, which has been detected as an important low-temperature combustion intermediate,[10] will undergo keto−enol tautomerization to acetaldehyde with an activation energy of 55.9 kcal mol^{-1}.[9] It has been demonstrated that the weakest bond in acetaldehyde is the $CH_3C(=O)-H$ bond,[8] making this hydrogen atom susceptible to abstraction by available radicals (especially at temperatures below 600 K),[11] yielding the resonantly stabilized acetyl radical ($CH_3C^{\bullet}=O$). The acetyl radical rapidly dissociates to CH_3 and CO, where the activation energy is only 17 kcal mol^{-1}.[12,13] This process provides a ready source of methyl radicals for methyl peroxy radical formation in low to moderate temperature thermal systems. Another route to methyl radical formation is by abstraction of the weak $CH_2=CHO-H$ hydrogen atom in vinyl alcohol, forming the resonantly stabilized vinoxy radical.[9] The vinoxy radical will then dissociate to give $CH_3 + CO$[12−14] via an initial intramolecular hydrogen shift forming the acetyl radical, with an activation energy of 40 kcal mol^{-1}.[12] Despite its potential importance, the self-reaction of the methyl peroxy radical has received relatively little attention in the combustion literature. Peroxy radical chemistry is especially important to ignition in the next generation of higher efficiency homogeneous charge compression ignition (HCCI) engines and pulse detonation engines (PDE).

Although there is essentially no experimental information on the enthalpy of formation or bond dissociation energies (BDEs) of dimethyl tetraoxide, many of these properties have been previously estimated from group additivity and semiempirical calculations. Using group additivity, Benson[15] finds the enthalpy of formation of $CH_3OOOOCH_3$ to be 6 ± 8 kcal mol^{-1}. Benson[15] also estimates enthalpies for the CH_3O, CH_3OO, and CH_3OOO radicals as 2 ± 2, 5.5 ± 3, and 24.5 ± 6 kcal mol^{-1}, respectively. Using the enthalpy values reported by Benson,[15] we calculate the $CH_3O-OOOCH_3$ BDE to be 20.5 kcal mol^{-1} and the $CH_3OO-OOCH_3$ BDE to be 5 kcal mol^{-1}. Later, Nangia and Benson[16] refined these group additivity values, resulting in an enthalpy for $CH_3OOOOCH_3$ of 3.6 kcal mol^{-1}, with enthalpies for CH_3O, CH_3OO, CH_3OOO, and CH_3OOOO of 3.9, 6.2, 23.0, and 39.8 kcal mol^{-1}. These updated group additivity values provide a $CH_3-OOOOCH_3$ BDE of 71.0 kcal mol^{-1} (using the experimental enthalpy of 34.82 kcal mol^{-1} for CH_3), a $CH_3O-OOOCH_3$ BDE of 23.3 kcal mol^{-1}, and a $CH_3OO-OOCH_3$ BDE of 8.8 kcal mol^{-1}. Lay and Bozzelli[17] derived new group additivity values of −5.5 and 9.6 kcal mol^{-1} for the O/C/O and O/O_2 groups, respectively. Using these group values with the recommended enthalpy for the $C/H_3/O$ group,[18] we now calculate the $CH_3OOOOCH_3$ enthalpy of formation as −11.8 kcal mol^{-1}, which is in serious disagreement with the previously reported group additivity values. Francisco and Williams[19] used semiempirical MNDO calculations to derive a group additivity value of 55 ± 6 kJ mol^{-1} (13.1 kcal mol^{-1}) for the O/O_2 group, and they used this value to calculate the enthalpy of formation of $CH_3OOOOCH_3$ to be −3.8 kcal mol^{-1}. Using MINDO/3 semiempirical calculations, Kokorev et al.[20] calculated the enthalpy of formation of $CH_3OOOOCH_3$ as 6.3 kcal mol^{-1}, which agrees relatively well with the values suggested by Benson[15] and Nangia and Benson.[16]

The radicals derived from dimethyl tetraoxide are of importance to atmospheric and combustion chemistry in their own right, and detailed thermochemistry for these species is of much usefulness. The radicals formed upon C−O and O−O bond dissociation in dimethyl tetraoxide are methyl (CH_3), methoxy (CH_3O), methlyperoxy (CH_3OO), methyltrioxy (CH_3OOO), and methyltetraoxy (CH_3OOOO). The importance of CH_3OO in atmospheric chemistry is established above, while the CH_3 and CH_3O radicals are both well-known combustion intermediates. Tetraoxy radicals such as CH_3OOOO are involved in stratospheric ozone destruction, as intermediates in reactions such as $CH_3O + O_3 \rightarrow CH_3OO + O_2$.[21] Similarly, trioxy radicals are implicated in ozone destruction through reactions of the type $CH_3 + O_3 \rightarrow CH_3O + O_2$.[22] The methyltrioxy radical has also been suggested as an intermediate in the atmospheric degradation of dimethyl sulfoxide.[23]

In this study we use high-level ab initio and density functional theory techniques to study the thermochemistry of dimethyl tetraoxide, due to its importance in the ozone cycle, as well as the possibly understated role that this molecule plays in low-temperature combustion processes. We calculate the molecule's standard enthalpy of formation ($\Delta_f H°_{298}$), entropy ($S°$), heat capacity as a function of temperature ($C_p(T)$), BDEs, and internal rotor potentials. Furthermore, we evaluate the abililty of a wide range of density functional theory methods to accurately calculate the thermochemical properties of $CH_3OOOOCH_3$ and its radicals. This study extends upon previous computational works on tetraoxide systems principally through its characterization of the internal rotor potentials for accurate $S°$ and $C_p(T)$ as well as by assessing a wider range of ab initio and density functional theory techniques. It is hoped that this work will provide valuable thermochemical input for use in the construction of accurate reaction models for the methyl peroxy radical, in both atmospheric and combustion processes.

Computational Methods

Optimized molecular geometries for $CH_3OOOOCH_3$, as well as its dissociation products CH_3OOOO, CH_3OOO, CH_3OO, CH_3O, and CH_3, have been calculated at the B3LYP/cc-pVTZ+d level of theory. In all cases, only the lowest energy conformer is considered, which is identified from an internal rotor analysis. Using the program SMCPS,[24] with B3LYP/cc-pVTZ+d geometries, frequencies, and moments of inertia, we calculate $S°_{298}$ and $C_p(T)$ values for each molecule. Entropy and heat capacity contributions from all internal rotors are explicitly considered using the program ROTATOR.[25] Here, relaxed scans of the dihedral angles corresponding to internal rotation were performed at the B3LYP/6-31G(d) density functional level, providing internal rotor potentials. These rotor potentials were fit with seven-parameter Fourier series expansions, which were used in the ROTATOR program to construct internal rotor Hamiltonians that were then solved to evaluate entropy and heat capacity contributions.[25] When calculating a molecule's entropy and heat capacity, the vibrational frequencies corresponding to

SCHEME 1: Isodesmic Reactions Used To Calculate the Enthalpy of Formation of $CH_3OOOOCH_3$

(1-1) $CH_3OOOOCH_3 + 3H_2O \rightarrow CH_3OCH_3 + 3H_2O_2$
(1-2) $CH_3OOOOCH_3 + 2H_2O \rightarrow 2CH_3OOH + H_2O_2$
(1-3) $CH_3OOOOCH_3 + 4H_2O \rightarrow 2CH_3OH + 3H_2O_2$
(1-4) $CH_3OOOOCH_3 + 4H_2O + CH_3CH_2CH_3 \rightarrow 2CH_3CH_2OH + 3H_2O_2 + CH_4$
(1-5) $CH_3OOOOCH_3 + 2H_2O \rightarrow CH_3OOCH_3 + 2H_2O_2$

TABLE 1: Reference Enthalpies Used in the Isodesmic Work Reactions of Schemes 1 and 2

	$\Delta_f H°_{298}$ (kcal mol^{-1})	reference
H_2O	-57.7978 ± 0.01	31
OH	9.319 ± 0.03	30
H_2O_2	-32.53 ± 0.05	30
HOO	2.94 ± 0.06	32
CH_4	-17.9 ± 0.1	33
$CH_3CH_2CH_3$	-25.02 ± 0.14	34
CH_3OH	-48.07 ± 0.05	35
CH_3O	4.42 ± 0.7	36
CH_3CH_2OH	-56.23 ± 0.12	37
CH_3OCH_3	-43.99 ± 0.12	38
CH_3OOCH_3	-30.0	39
CH_3OOH	-31.31 ± 1.2	40

SCHEME 2: Isodesmic Reactions Used To Calculate the C−O and O−O BDEs in $CH_3OOOOCH_3$

Bond	Reaction
CH_3—$OOOOCH_3$	(2-1) $CH_3OOOOCH_3 + CH_3O \rightarrow CH_3OCH_3 + CH_3OOOO$
	(2-2) $CH_3OOOOCH_3 + HOO \rightarrow CH_3OH + CH_3OOOO$
	(2-3) $CH_3OOOOCH_3 + OH \rightarrow CH_3OH + CH_3OOOO$
CH_3O—$OOOCH_3$	(2-4) $CH_3OOOOCH_3 + 2OH \rightarrow CH_3O + CH_3OOO + H_2O_2$
	(2-5) $CH_3OOOOCH_3 + OH \rightarrow CH_3OOO + CH_3OOH$
CH_3OO—$OOCH_3$	(2-6) $CH_3OOOOCH_3 + 2OH \rightarrow 2CH_3OO + H_2O_2$
	(2-7) $CH_3OOOOCH_3 + CH_3O + OH \rightarrow 2CH_3OO + CH_3OOH$

internal rotation were omitted from the SMCPS calculations, with the ROTATOR corrections added to the final values. Hindered internal rotor corrections to entropy values are also calculated using the formalism of Ayala and Schlegel,[26] as implemented in Gaussian 03.

Accurate enthalpies of formation and bond dissociation energies are determined using the composite theoretical methods G3B3[27] and CBS-APNO.[28] Isodesmic work reactions are used to minimize systematic calculation errors;[7,29] these isodesmic enthalpies are validated against atomization enthalpies, which we calculate using the C, O, and H enthalpies of the National Institute of Science and Technology−Joint Army Navy Air Force tables.[30] The isodesmic work reactions used for $CH_3OOOOCH_3$ are listed in Scheme 1; the reference species utilized in these reactions are listed in Table 1, along with their experimentally determined enthalpies of formation. Bond dissociation energies are also calculated using isodesmic work reactions, as well as using the non-isodesmic bond dissociation reactions. The isodesmic reactions used to determine bond energies for each of the O−O and C−O bonds in $CH_3OOOOCH_3$ are provided in Scheme 2, and enthalpies of formation for the reference species are included in Table 1. In addition, enthalpies of formation for each of the radicals corresponding to dissociation of the $CH_3OOOOCH_3$ radical are calculated from the enthalpy of formation of $CH_3OOOOCH_3$ and the individual BDEs. These enthalpy values are also compared with atomization enthalpies. All ab initio and density functional calculations were performed with the Gaussian 03 program.[41] Molecular geometries (in Cartesian coordinates) and enthalpies (in hartrees) for $CH_3OOOOCH_3$ and its radicals are provided in the Supporting Information.

The enthalpy of formation of dimethyl tetraoxide, and its BDEs have been calculated using a variety of density functional theory (DFT) methods, from atomization reactions and with the isodesmic reaction schemes outlined above. We have selected the DFT methods B3LYP,[42] TPSS,[43] PBE0[44] (otherwise known as PBE1PBE or PBEh), O3LYP,[42b,45] BMK,[46] B98,[47] B1B95,[42a,48] VSXC,[49] TPSSh,[43,50] and X3LYP.[42b,51] for evaluation. Molecular geometries for each method were optimized with the 6-31G(d) basis set. Higher-level single-point energy corrections were then applied with the 6-311++G(3df,3pd) basis set.

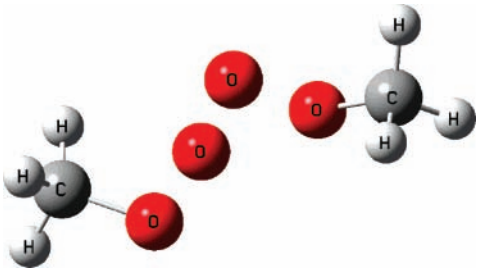

Figure 1. Molecular geometry of $CH_3OOOOCH_3$ at the B3LYP/cc-pVTZ+d level of theory.

Results and Discussion

Molecular Geometries and Internal Rotor Potentials. Figure 1 illustrates the optimized B3LYP/cc-pVTZ+d geometry for $CH_3OOOOCH_3$, while Figure 2 shows the B3LYP/cc-pVTZ+d geometries of the CH_3OOOO, CH_3OOO, and CH_3OO radicals. Additionally, C−O and O−O bond lengths for each of these species and the methoxy radical are listed in Table 2 along with B3LYP/6-31G(d) and QCISD/6-311G(d,p) bond lengths from the G3B3 and CBS-APNO calculations, respectively. It is interesting to note that at both levels of theory the $CH_3OOOO^{\bullet}$ radical is predicted to exist as a loosely bound complex between a methoxy radical and molecular oxygen, with the QCISD calculations predicting a significantly longer CH_3OO-OO bond length. However, there is generally good agreement between the B3LYP and the QCISD geometrical parameters, with differences being typically 0.02 Å or less, as illustrated in Table 2. Comparatively, Ghigo et al.[4b] obtained bond lengths of 1.406, 1.474, and 1.413 Å for the respective C−O, CO−O, and OO−OO bonds in dimethyl tetraoxide from complete active space multiconfiguration self-consistent field (CAS-MCSCF) calculations. These values are within satisfactory agreement of our B3LYP and QCISD bond lengths, although in the multireference CAS-MCSCF calculations there is some contraction of the two C−O bonds (ca. 0.02 Å) and lengthening of the two CO−O bonds (ca. 0.04 Å). This may be related to admixing of a low-energy triplet structure in the dimethyltetraoxide ground state, such as $CH_3O-O_2-CH_3O$.

The internal rotor potentials for motion about the $CH_3OO-OOCH_3$, $CH_3O-OOOCH_3$, and $CH_3-OOOOCH_3$ bonds in dimethyl tetraoxide have been calculated from relaxed scans of the corresponding dihedral angles at the B3LYP/6-31G(d) level of theory. The $CH_3-OOOOCH_3$ rotor is depicted in Figure 3; this rotor occurs twice in $CH_3OOOOCH_3$ and exhibits a barrier to internal rotation of ca. 2.5 kcal mol^{-1}, with 3-fold symmetry. The minimum for $O-CH_3$ rotation is the result of a favorable dipole−dipole interaction between the H atom and the electronegative oxygen atom bonded to the methyl carbon. This is illustrated in Figure 4, where the electrostatic potential for dimethyl tetraoxide has been mapped onto the total electron density isosurface.

The $CH_3O-OOOCH_3$ rotor potential is depicted in Figure 5. This rotor occurs twice in dimethyl tetraoxide, with an asymmetrical barrier and with two minima. In both minima the

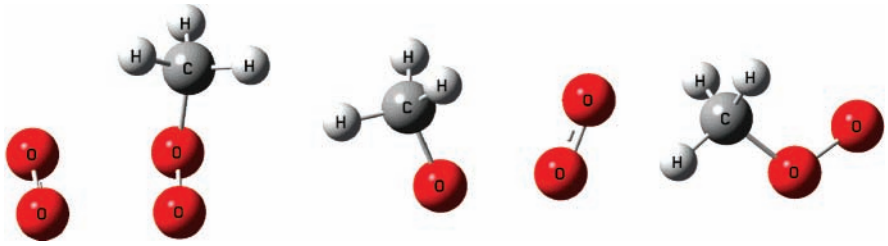

Figure 2. Molecular geometries of the CH_3OOOO, CH_3OOO, and CH_3OO radicals (from left to right) at the B3LYP/cc-pVTZ+d level of theory.

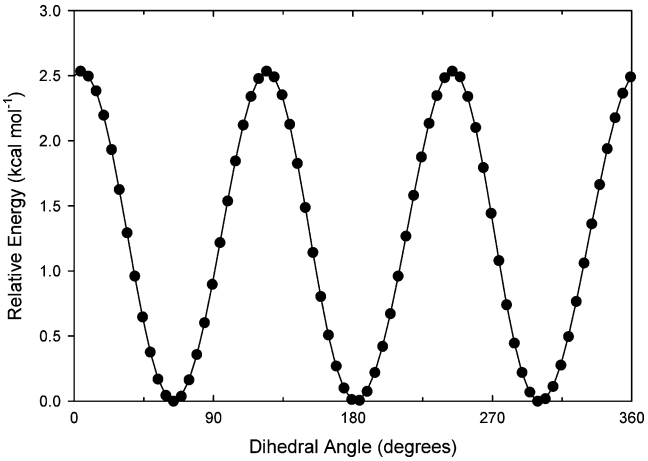

Figure 3. $CH_3-OOOOCH_3$ internal rotor potential, calculated at the B3LYP/6-31G(d) level.

TABLE 2: Bond Lengths (Å) in $CH_3OOOOCH_3$ and Its Radicals at the B3LYP/6-31G, B3LYP/cc-pVTZ+d, and QCISD/6-311G(d,p) Theoretical Levels

	B3LYP/ 6-31G(d)	B3LYP/ cc-pVTZ+d	QCISD/ 6-311G(d,p)
	$CH_3OOOOCH_3$		
$CH_3-OOOOCH_3$	1.4266	1.4249	1.4254
$CH_3O-OOOCH_3$	1.4351	1.4311	1.4156
$CH_3OO-OOCH_3$	1.4231	1.4169	1.4082
	$CH_3OOOO^{\bullet}$		
CH_3-OOOO	1.4487	1.4467	1.4411
CH_3O-OOO	1.3228	1.3170	1.3241
CH_3OO-OO	2.8730	3.0818	3.3685
CH_3OOO-O	1.2146	1.2057	1.2020
	$CH_3OOO^{\bullet}$		
CH_3-OOO	1.4020	1.3987	1.4222
CH_3O-OO	1.5829	1.5891	1.4832
CH_3OO-O	1.2472	1.2355	1.2711
	$CH_3OO^{\bullet}$		
CH_3-OO	1.4483	1.4465	1.4409
CH_3O-O	1.3228	1.3171	1.3241
	$CH_3O^{\bullet}$		
CH_3-O	1.3686	1.3627	1.379

rotating CH_3O moiety is in a gauche conformation, with C−O−O−O dihedral angles of ca. 90° and 270°. The energy difference between the two minima is almost negligible (<1 kcal mol^{-1}). The maximum barrier for rotation occurs with a barrier of around 6 kcal mol^{-1}, with this rotational transition state corresponding to a cis geometry (C−O−O−O dihedral ∼0°). The second, lower-energy, rotational transition state exhibits a trans geometry (C−O−O−O dihedral ∼180°), with barrier of ca. 4 kcal mol^{-1}. The favored gauche conformation across peroxy bonds (RO−OR) is well-known in the literature.[52]

The final rotor potential for dimethyl tetraoxide, corresponding to $CH_3OO-OOCH_3$ internal rotation, is illustrated in Figure 6. This rotor demonstrates an asymmetric 2-fold potential, with a maximum barrier for rotation of ca. 7 kcal mol^{-1}. There exist

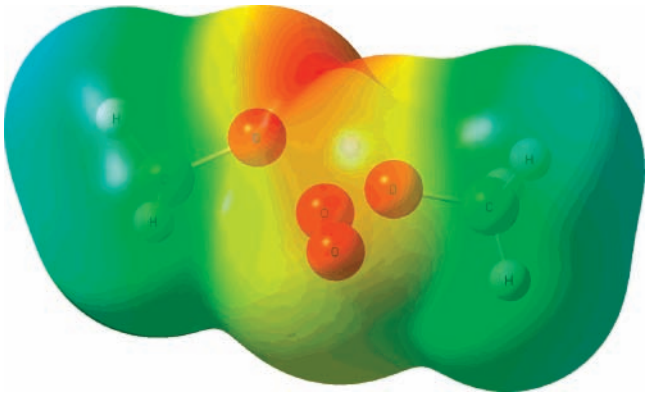

Figure 4. Electrostatic potential mapped onto the total electron density isosurface for $CH_3OOOOCH_3$: red, −0.04764; green, neutral; dark blue, 0.04764.

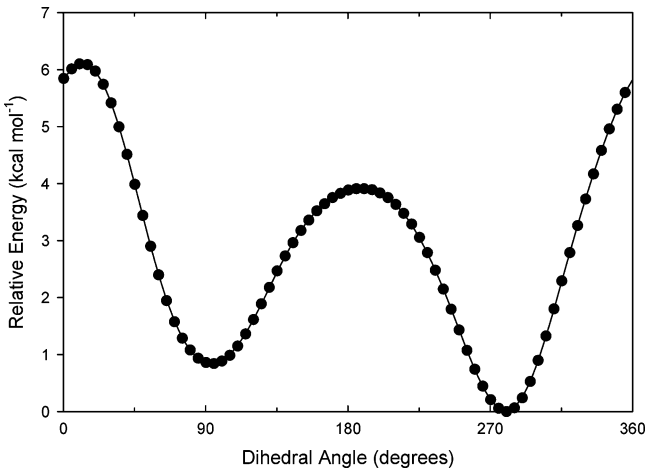

Figure 5. $CH_3O-OOOCH_3$ internal rotor potential, calculated at the B3LYP/6-31G(d) level.

two minima, both gauche and 2.5 kcal mol^{-1} different in energy. In the global minima the methyl groups are directed away from each other, while in the less-stable conformer the methyl groups are directed toward each other. Increased steric and electrostatic interaction between the methyl groups explains the ca. 3 kcal mol^{-1} energy difference between the two rotational isomers. There exist two rotational transition states on the $CH_3OO-OOCH_3$ potential energy surface of a similar energy, corresponding to the cis and trans geometries. A small inflection also exists near the trans rotational transition state; this is not considered further here. The cis transition state is more staggered than the trans transition state, with respective O−O−O−O dihedral angles of 27.4° (vs 0° in the fully cis structure) and 162.6° (vs 180° in the fully trans structure).

As shown above, the energy required for internal rotation about peroxy bonds in dimethyl tetraoxide is significantly greater than that required for rotation about the two $CH_3-OOOOC$ bonds. Internal motions about the three peroxy bonds may therefore be best described as vibrational frequencies and not

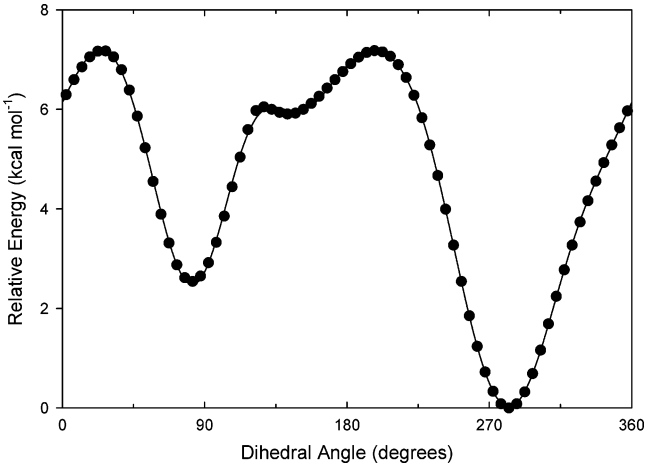

Figure 6. $CH_3OO-OOCH_3$ internal rotor potential, calculated at the B3LYP/6-31G(d) level.

as hindered internal rotors. This is especially true given that the weakly bound dimethyl tetraoxide molecule will only exist at low to moderate temperatures, where the vibrational energy may be too low for rotation about the O−O single bonds. Furthermore, significant coupling of the peroxy rotors is also expected, where internal motion of the molecule in three-dimensional space contributes to rotation about two or more bonds. Full treatment of the three peroxy rotors according to the one-dimensional rotor potentials calculated in this study would therefore result in an overestimation of the molecule's entropy and heat capacity. This effect should increase with the number of internal rotors and should become even more significant in dimethyl tetraoxide than in the methyl polyoxy radicals.

Internal rotor potentials for the CH_3OO, CH_3OOO, and CH_3OOOO radicals are provided as Supporting Information. We were not able to determine contiguous rotor energy profiles for CH_3O-OOO and CH_3OO-OO rotors with relaxed scans. We initially performed rigid scans of the rotor potentials, followed by geometry optimizations at 30° intervals (over only 180° for CH_3O-OOO, using 2-fold symmetry), with the respective dihedral angles frozen. As in dimethyl tetraoxide, the $O-CH_3$ internal rotors exhibit 3-fold potentials with low-energy barriers (<1 kcal mol^{-1}). However, for rotation about O−O bonds in these radicals we find rotational barriers of 3 kcal mol^{-1} and below. We therefore suggest that all rotors in the methyl polyoxy radicals be treated as hindered internal rotors and not as vibrational frequencies. Rotor coupling in these radical species should also be less important than that in dimethyl tetraoxide, further supporting this approach.

Entropy and Heat Capacity. Entropy ($S°_{298}$) and heat capacity ($C_p(T)$) values have been determined for $CH_3OOOOCH_3$ and its radicals CH_3OOOO, CH_3OOO, CH_3OO, and CH_3O using B3LYP/cc-pVTZ+d geometries, moments of inertia, and vibrational frequencies. Heat capacity values have been calculated over the temperature range from 300 to 1500 K. Entropy values for $CH_3OOOOCH_3$, CH_3OOOO, CH_3OOO, CH_3OO, and CH_3O are obtained using several different approaches to treat the internal rotational modes, and the results are presented in Table 3. First, we present the rigid-rotor-harmonic-oscillator (RRHO) entropies, in which all modes are treated as vibrational frequencies. Following this we present entropies determined using the internal rotor contributions calculated using the ROTATOR program with (a) only the methyl internal rotors and (b) using all internal rotors. Our recommended entropy values, where we treat only the methyl internal rotors in dimethyl tetraoxide and all internal rotors in the remaining species using ROTATOR, are listed in bold. Heat capacities calculated with the recommended rotor treatment, for $T = 300-1500$ K, are provided in Table 4 along with recommended values of $S°_{298}$ and the point group symmetry of each species. Finally, for comparative purposes we also present entropies adjusted for internal rotation using the formalism of Ayala and Schlegel (A & S), as implemented in Gaussian 03. Entropies are provided for the three different internal rotor corrections available under this internal rotor scheme, i.e., Truhlar,[53] Pitzer and Gwinn,[54] and "best fit".[41] These three methods use different correlations to approximate the hindered rotor partition function, which lies between the limiting free rotor and harmonic oscillator values.

In Table 3 we find that the entropy of $CH_3OOOOCH_3$ varies considerably with the different methods of treating the internal rotors. All of the methods find the entropy to be several cal mol^{-1} K^{-1} greater than the RRHO value, demonstrating that proper treatment of the internal rotors is important. The recommended ROTATOR entropy agrees relatively well with the A & S values, with differences of between 1.4 and 2.4 cal mol^{-1} K^{-1}. However, when all of the internal rotors in $CH_3OOOOCH_3$ are treated using ROTATOR we find an entropy value that is ca. 6−8 cal mol^{-1} K^{-1} greater than the other values and believe this is an overestimation of the molecular entropy due to the significant coupling of the internal rotational modes. For the radicals CH_3OOOO, CH_3OOO, and CH_3OO proper treatment of the internal rotors provides a smaller, but still significant, correction to the entropy over the RRHO values. This is due to the presence of only one low-energy methyl rotational mode in these radical species. We also see that the ROTATOR entropies calculated using only the methyl internal rotors agree very well with those calculated using all internal rotors, which suggests a much lesser degree of coupling for these species than in $CH_3OOOOCH_3$. For CH_3OO, the A & S entropies are very similar to the RRHO values. For CH_3OOOO the A & S calculation failed, while for CH_3OOO it provided entropy corrections that are clearly unrealistic. The reason for the failure of the A & S rotor treatment in these radicals is unknown but might be related to incorrect identification of the molecular connectivity and/or the internal rotational modes.

Enthalpy of Formation of $CH_3OOOOCH_3$. Reaction enthalpies for the isodesmic work reactions of Scheme 1 have been calculated with the G3B3 and CBS-APNO methods and are listed in Table 5, along with the enthalpies of formation obtained with each reaction. We find that the reaction enthalpies are relatively small, indicating good cancellation of bond energy across the work reactions. The enthalpies calculated with the two theoretical methods agree to within 0.5 kcal mol^{-1} for all five work reactions. The enthalpies of formation obtained with reaction 1-2 in Scheme 1 are, on average, 0.7 kcal mol^{-1} smaller than the values obtained with the other work reactions. This could be the result of a small error in the enthalpy of formation of CH_3OOH (which is the only unique species in this work reaction), where the experimental enthalpy of −31.31 kcal mol^{-1} is too low by 0.3−0.4 kcal mol^{-1}, with the correct value therefore being ca. −31.0 kcal mol^{-1}. There is some support in the literature for this assertion, where the 298 K enthalpy of formation of CH_3OOH has been calculated as −30.4, −30.7, and −30.75 kcal mol^{-1} with the respective CCSD(T)/CBS, CBS-APNO, and CBS-Q theoretical methods.[55]

Table 6 lists the average isodesmic enthalpies of formation for the two theoretical methods, compared to enthalpy values obtained using an atomization work reaction. Comparatively,

TABLE 3: Entropies (cal mol^{-1} K^{-1}) for $CH_3OOOOCH_3$ and Its Radicals, Calculated Using Different Internal Rotor Treatments, at the B3LYP/cc-pVTZ+d Level of Theory[a]

	$CH_3OOOOCH_3$	CH_3OOOO	CH_3OOO	CH_3OO	CH_3O
RRHO[b]	83.53	95.66	71.37	64.30	**56.64**
methyl rotor(s)[c]	**88.13**	96.58	73.95	66.86	
all rotors[d]	93.77	**96.76**	**75.89**	**66.86**	
Ayala and Schlegel (T)[e]	85.69		−11.60	64.09	
Ayala and Schlegel (PG)[e]	86.70		−11.60	64.52	
Ayala and Schlegel (BF)[e]	86.61			64.51	

[a] Recommended values are listed in bold. [b] All vibrational modes treated as frequencies using the RRHO approximation. [c] Methyl internal rotors are treated using the ROTATOR program. [d] All internal rotors are treated using the ROTATOR program. [e] RRHO entropies are corrected according to the formalism of Ayala and Schlegel as implemented in Gaussian 03, using the corrections of Truhlar (T), Pitzer and Gwinn (PG), and the "best fit" (BF) values.[26]

TABLE 4: Recommended Entropies and Heat Capacities (cal mol^{-1} K^{-1}) and Symmetry Point Groups for $CH_3OOOOCH_3$ and Its Radicals from B3LYP/cc-pVTZ+d Calculations

	point group	$S°_{298}$	$C_p(300)$	$C_p(400)$	$C_p(500)$	$C_p(600)$	$C_p(800)$	$C_p(1000)$	$C_p(1500)$
$CH_3OOOOCH_3$	C_2	88.13	27.46	32.58	36.95	40.59	46.20	50.31	56.68
CH_3OOOO	C_1	96.76	22.69	25.05	27.06	28.68	31.05	32.71	35.23
CH_3OOO	C_s	75.89	17.61	19.58	21.43	23.10	25.87	27.96	31.23
CH_3OO	C_s	66.86	12.02	14.06	16.11	17.91	20.78	22.90	26.20
CH_3O	C_1	56.64	9.83	11.57	13.24	14.71	17.12	18.95	21.84

TABLE 5: Isodesmic Reaction Enthalpies and Enthalpies of Formation of $CH_3OOOOCH_3$ Determined Using Isodesmic Work Reactions

	$\Delta_{rxn}H°$ (kcal mol^{-1})		$\Delta_fH°$ (kcal mol^{-1})	
reaction[a]	G3B3	CBS-APNO	G3B3	CBS-APNO
1-1	41.18	41.27	−9.37	−9.46
1-2	30.68	30.95	−10.23	−10.50
1-3	46.82	47.03	−9.36	−9.57
1-4	37.75	38.21	−9.49	−9.95
1-5	30.52	30.79	−9.99	−10.25

[a] Reaction numbers correspond to those of Scheme 1.

TABLE 6: Enthalpies of Formation of $CH_3OOOOCH_3$ Determined Using Isodesmic and Atomization Reactions

		$\Delta_fH°$ (kcal mol^{-1})
isodesmic	G3B3	−9.7
work	CBS-APNO	−9.9
reactions	average	−9.8
atomization	G3B3	−8.0
work	CBS-APNO	−9.3
reactions	average	−8.7

there is a ca. 1 kcal mol^{-1} difference between the isodesmic and the atomization enthalpies. From the above calculations, we recommend a value of −9.8 kcal mol^{-1} for $CH_3OOOOCH_3$, which is an average of the isodesmic values obtained with the CBS-APNO and G3B3 theoretical methods. Comparing this value to previous group additivity estimates, we find that the earlier group additivity and semiempirical values (6 ± 8,[15] 3.6,[16] and 6.3[20] kcal mol^{-1}) are in significant error, while the more recent values (−11.8[18] and −3.8[19] kcal mol^{-1}) agree with our calculated enthalpy, at least to the degree expected for group additivity approximations.

Bond Dissociation Energies. Bond dissociation energies for the C−O and O−O bonds in $CH_3OOOOCH_3$ have been calculated with the G3B3 and CBS-APNO theoretical methods, using isodesmic and bond dissociation work reactions, as discussed in the Computational Methods section. Table 7 lists the isodesmic reaction enthalpies and the BDEs obtained using these isodesmic work reactions. We find that all of the bonds are relatively weak, especially the O−O bonds. Interestingly, the isodesmic reaction enthalpies are of a similar value to, and usually greater than, the bond energies. Therefore, the use of bond dissociation work reactions should provide more accurate BDEs than our isodesmic work reaction, as there should be a greater degree of bond error cancellation, while also making use of more accurately known reference enthalpies. The isodesmic work reactions will still offer some advantages over the bond dissociation work reactions, such as conservation of electron spin (leading to cancellation of spin contamination) and conservation of the number of molecular fragments (leading to cancellation in the basis set superposition error). The BDE values obtained for the G3B3 and CBS-APNO methods using bond dissociation work reactions are listed in Table 8, along with the average BDEs from isodesmic reaction analysis. In Table 8 we see that the average BDEs suggested by each method agree to within 1.5 kcal mol^{-1}, which reflects the higher degree of error associated with these calculations relative to those for the closed-shell molecule $CH_3OOOOCH_3$. Based upon the results presented in Table 8, we recommend a $CH_3-OOOOCH_3$ BDE of 46.0 kcal mol^{-1}, a $CH_3O-OOOCH_3$ BDE of 20.0 kcal mol^{-1}, and a $CH_3OO-OOCH_3$ BDE of 13.9 kcal mol^{-1}. We estimate the uncertainty of these bond energies to be ca. 2 kcal mol^{-1}.

TABLE 7: Isodesmic Reaction Enthalpies and BDEs for $CH_3OOOOCH_3$ Determined Using Isodesmic Reactions

	$\Delta_{rxn}H°$ (kcal mol^{-1})		BDE (kcal mol^{-1})	
reaction[a]	G3B3	CBS-APNO	G3B3	CBS-APNO
		$CH_3-OOOOCH_3$		
2-1	−38.12	−37.83	45.11	45.40
2-2	−22.89	−21.44	46.18	47.63
2-3	−45.78	−45.63	46.42	46.58
		$CH_3O-OOOCH_3$		
2-4)	−30.37	−28.48	20.80	22.69
2-5	−25.14	−22.95	19.91	22.10
		$CH_3OO-OOCH_3$		
2-6	−34.25	−36.74	16.92	14.43
2-7	−29.01	−31.21	16.03	13.84

[a] Reaction numbers correspond to those of Scheme 1.

Using reference enthalpies for CH_3 and CH_3O and our calculated $CH_3OOOOCH_3$ enthalpy, we can use our recommended BDEs to determine enthalpies of formation for the CH_3OO, CH_3OOO, and CH_3OOOO radicals. Table 9 lists our

TABLE 8: $CH_3OOOOCH_3$ BDEs Determined Using Isodesmic and Atomization Work Reactions

		BDE (kcal mol^{-1})	
		isodesmic work reactions	bond dissociation work reactions
$CH_3-OOOOCH_3$	G3B3	45.9	45.1
	CBS-APNO	46.5	46.8
	average	46.2	46.0
$CH_3O-OOOCH_3$	G3B3	20.4	18.3
	CBS-APNO	22.4	21.7
	average	21.4	20.0
$CH_3OO-OOCH_3$	G3B3	16.5	14.4
	CBS-APNO	14.1	13.4
	average	15.3	13.9

TABLE 9: Recommended $CH_3OOOOCH_3$ BDEs and Enthalpies of Formation ($\Delta_fH°_{298}$) for the CH_3OO, CH_3OOO, and CH_3OOOO Radicals[a]

	BDE[b]		$\Delta_fH°_{298}$[c]
$CH_3-OOOOCH_3$	46.0	CH_3OO	2.1
$CH_3O-OOOCH_3$	20.0	CH_3OOO	5.8
$CH_3OO-OOCH_3$	13.9	CH_3OOOO	1.4

[a] All values are given in kcal mol^{-1}. [b] Average of CBS-APNO and G3B3 calculations, using bond dissociation work reactions. [c] From calculated BDEs and $CH_3OOOOCH_3$ enthalpy, using experimental CH_3 and CH_3O enthalpies.

TABLE 10: Literature Group Additivity Values for the O/O_2 Group Enthalpy[a]

	O/O_2 enthalpy
Benson[15]	17.5
Nangia and Benson[16]	16.3
Kokorev et al.[20]	17.7
Francisco and Williams[19]	13.1
Lay and Bozzelli[17]	9.6
this study	9.6

[a] All values are given in kcal mol^{-1}.

recommended enthalpies for each of these radicals, as well as the recommended BDEs.

Calculated BDEs for dimethyltetraoxide have been previously reported in the literature, and provide a comparison with our recommended bond energies. Ghigo et al. [4b] reported reaction enthalpies for the $2CH_3OO \rightarrow CH_3OOOOCH_3$ and the $2CH_3OO \rightarrow CH_3O + CH_3OOO$ reactions at the CAS-PT2/6-311G(2df,p), CBS-Q, and G2 levels. They obtained BDEs of 12.8, 15.0, and 9.2 kcal mol^{-1} for the $CH_3OO-OOCH_3$ bond and 21.5, 24.0, and 19.1 kcal mol^{-1} for the $CH_3O-OOOCH_3$ bond, with the CBS-Q, G2, and CAS-PT2 methods, respectively. These values compare well with our respective BDEs of 13.9 and 20.0 kcal mol^{-1}.

Group Additivity Values. Our new calculation of the enthalpy of formation of $CH_3OOOOCH_3$ allows us to redetermine the important O/O_2 group additivity value. Using group additivity, the enthalpy of formation of $CH_3OOOOCH_3$ is calculated from eq 8, using the $C/H_3/O$, O/C/O and O/O_2 groups. While the $C/H_3/O$ and O/C/O group enthalpy values are now relatively well-established, that of O/O_2 is not. Using the $C/H_3/O$ and O/C/O group values of Cohen and Benson[18] (−10.0 and −4.5 kcal mol^{-1}, respectively), we calculate the O/O_2 group enthalpy to be 9.6 kcal mol^{-1}. Table 10 compares this group enthalpy value to some previous estimates. We see that over time the O/O_2 group enthalpy has generally decreased, converging toward our recommended value

$$\Delta_fH°\ (CH_3OOOOCH_3) = 2C/H_3/O + 2O/C/O + 2O/O_2 \quad (8)$$

Similar group additivity calculations have been performed for $S°_{298}$ and $C_p(T)$ of the O/O_2 group in $CH_3OOOOCH_3$. For the $C/H_3/O$ and O/C/O groups, we have utilized the group additivity values of Benson[56] and Lay,[57] respectively. The resultant $S°_{298}$ and $C_p(T)$ values determined for the O/O_2 group and reference values for the $C/H_3/O$ and O/C/O groups are presented in Table 11.

Density Functional Theory Calculations. Density functional theory can provide a relatively inexpensive means of accurately calculating thermochemical properties. This can be especially useful for large systems, which may not render themselves suitable to study with more computationally intensive theoretical methods, such as those employed in our above calculations. The organic tetraoxides formed from alkyl peroxy radicals larger than the methyl peroxy radical may constitute such molecules, and it is therefore useful to identify which DFT methods are best suited to studying these systems. It is important to note, however, that the hybrid DFT methods may introduce some systematic error when moving to systems with increasingly large alkyl substituents.[58] In addition the recent literature includes a number of new density functionals now available to the computational chemist; the benchmarking of these functionals with a diverse range of molecules, featuring an array of bonding environments, is of value. It is particularly important to evaluate the DFT methods designed for accurate thermodynamics of transition states and for properties of molecules featuring weak bonds with significant long-range nonbonded interactions. Density functional theory traditionally has been criticized as poor for these systems. The $CH_3OOOOCH_3$ molecule and its radicals provide us with a very good opportunity to study some of these newer DFT methods.

We have chosen to use the DFT methods B3LYP, TPSS, PBE0, O3LYP, BMK, B98, B1B95, VSXC, TPSSh, and X3LYP. These methods present an assortment of density functionals, including several that were either designed for, or have demonstrated accuratacy in, studies on some transition states and other weakly bonded molecules (i.e., BMK,[46] B98,[59] B1B95,[59,60] TPSS(h),[50] and PBE0[59]). We also include a mix of hybrid and nonhybrid functionals, while also including several generalized gradient approximation (GGA) and meta-GGA methods. Geometry optimization and frequency calculations are performed for all methods using the double-ζ 6-31G(d) basis set. Single-point energies, based upon 6-31G(d) geometries, are also obtained for each DFT method using the 6-311++G(3df,3pd) basis set; this is a larger triple-ζ basis set, augmented with diffuse and polarization functions.

Table 12 lists enthalpies of formation calculated for $CH_3OOOOCH_3$, CH_3OOOO, CH_3OOO, CH_3OO, and CH_3O using atomization work reactions with each of the DFT methods and basis sets. Also included are errors, relative to the enthalpy values recommended in this study (and a literature enthalpy of 4.42 kcal mol^{-1} for CH_3O), as well as an average error across each combination of density functional and basis set. As we are using calculated values for reference enthalpies, we feel that we are not able to discriminate the error of the density functional calculations to less than ±2 kcal mol^{-1}. From Table 12, we find that the best-performed functionals for enthalpies of formation from atomization reactions with the 6-31G(d) basis set are BMK, B1B95, PBE0, and B98, while with the larger basis set the most successful methods are B1B95, TPSSh, X3LYP, and PBE0. In general, the DFT methods designed to

TABLE 11: Group Additivity Values for Entropy ($S°_{298}$) and Heat Capacity ($C_p(T)$) in $CH_3OOOOCH_3$[a]

	$S°_{298}$	C_p(300)	C_p(400)	C_p(500)	C_p(600)	C_p(800)	C_p(1000)	C_p(1500)	reference
C/H$_3$/O	30.41	6.19	7.84	9.40	10.79	13.03	14.77	17.58	Benson[56]
O/C/O	8.54	3.90	4.31	4.60	4.84	5.32	5.80	6.47	Lay[57]
O/O$_2$	5.12	3.64	4.14	4.48	4.67	4.75	4.59	4.29	this study

[a] All values are given in cal mol^{-1} K^{-1}.

TABLE 12: Enthalpy of Formation of $CH_3OOOOCH_3$ and Its Radicals CH_3OOOO, CH_3OOO, CH_3OO, and CH_3O from Atomization Work Reactions, Using 10 DFT Methods with the 6-31G(d) and 6-311++G(3df,3pd) Basis Sets[a]

		$CH_3OOOOCH_3$		CH_3OOOO		CH_3OOO		CH_3OO		CH_3O		mean absolute
		$\Delta_fH°_{298}$	error	$\Delta_fH°_{298}$	error	$\Delta_fH°_{298}$	error	$\Delta_fH°_{298}$	error	$\Delta_fH°_{298}$	error	error
B3LYP	6-31G(d)	−10.1	0.3	−4.8	6.2	1.3	4.5	−0.7	2.8	2.0	2.4	3.2
	6-311++G(3df,3pd)	−5.5	4.3	−2.4	3.8	3.7	2.1	−0.2	2.3	0.8	3.6	3.2
TPSS	6-31G(d)	−34.6	24.8	−19.5	20.9	−18.3	24.1	−10.2	12.3	−3.0	7.4	17.9
	6-311++G(3df,3pd)	−28.1	18.3	−14.2	15.6	−14.8	20.6	−8.8	10.9	−3.5	7.9	14.7
PBE0	6-31G(d)	−8.6	1.2	−3.8	5.2	3.3	2.5	0.2	1.9	2.7	1.7	2.5
	6-311++G(3df,3pd)	−7.0	2.8	−3.5	4.9	3.9	1.9	−0.2	2.3	1.4	3.0	3.0
O3LYP	6-31G(d)	−17.8	8.0	−15.2	16.6	−7.0	12.8	−5.4	7.5	−1.4	5.8	10.1
	6-311++G(3df,3pd)	−10.0	0.2	−10.9	12.3	−2.6	8.4	−3.3	5.4	−1.1	5.5	6.4
BMK	6-31G(d)	−4.0	5.8	2.2	0.8	9.5	3.7	2.2	0.1	4.2	0.2	2.1
	6-311++G(3df,3pd)	−5.8	4.0	12.2	10.8	8.7	2.9	0.3	1.8	1.1	3.3	4.6
B98	6-31G(d)	−9.5	0.3	−5.2	6.6	2.1	3.7	0.0	2.1	3.4	1.0	2.7
	6-311++G(3df,3pd)	−7.1	2.7	−4.3	5.7	3.3	2.5	−0.1	2.2	2.2	2.2	3.1
B1B95	6-31G(d)	−5.6	4.2	−2.9	4.3	4.7	1.1	1.2	0.9	3.7	0.7	2.2
	6-311++G(3df,3pd)	−2.6	7.2	−1.3	2.7	6.2	0.4	1.4	0.7	3.0	1.4	2.5
VSXC	6-31G(d)	−21.4	11.6	−18.3	19.7	−10.5	16.3	−0.7	2.8	2.1	2.3	10.5
	6-311++G(3df,3pd)	−13.4	3.6	−14.2	15.6	−6.6	12.4	1.3	0.8	2.4	2.0	6.9
TPSSh	6-31G(d)	−13.3	3.5	−1.7	3.1	−0.7	6.5	−1.4	3.5	0.4	4.0	4.1
	6-311++G(3df,3pd)	−9.6	0.2	−0.4	1.8	1.6	4.2	−1.0	3.1	−0.5	4.9	2.8
X3LYP	6-31G(d)	−10.8	1.0	−4.9	6.3	1.6	4.2	−0.9	3.0	1.7	2.7	3.4
	6-311++G(3df,3pd)	−6.0	3.8	−1.8	3.2	4.3	1.5	−0.2	2.3	0.7	3.7	2.9

[a] All values are given in kcal mol^{-1}.

study reaction kinetics outperformed those that are not. Furthermore, there is in general no significant improvement obtained by moving to the larger 6-311++G(3df,3pd) basis set. The poorest performing methods for these atomization reactions are TPSS, O3LYP, and VSXC across both basis sets.

Analyzing only the radicals of Table 12, we find that many of the DFT methods exhibit poor size consistency, as there is a general trend of increasing error with increasing molecular size. This is illustrated in Figure 7, where the number of heavy atoms in a molecule is plotted against the computational error for each of the DFT methods for the 6-311++G(3df,3pd) basis set. (Similar results are obtained with the 6-31G(d) basis set.). The DFT methods exhibiting the worst size consistency (TPSS, O3LYP, and VSXC) are, not surprisingly, those that provided the largest average errors from our atomization calculations. The poor size consistency of these DFT methods for radical species could be related to spin contamination, which would explain why the closed-shell molecule $CH_3OOOOCH_3$ does not follow the same trend as the open-shell species. Values of the spin operator (S^2) are tabulated for each of the radicals in the Supporting Information, and we do find that S^2 generally increases with increasing molecular size. Spin contamination is not, however, larger for the less accurate DFT methods. This may be an indication that the DFT methods TPSS, O3LYP, and VSXC are particularly affected by spin contamination. We also note that spin contamination is large in CH_3OOOO but relatively unimportant in the remaining radicals.

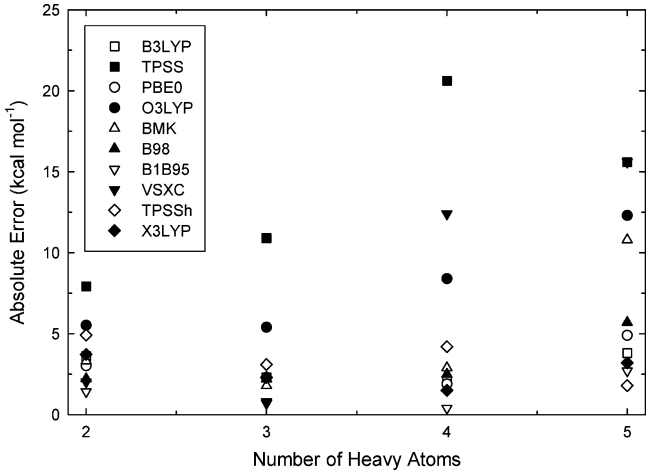

Figure 7. Relationship between molecular size and absolute error for DFT atomization calculations on the radicals corresponding to C−O and O−O bond cleavage in $CH_3OOOOCH_3$, with the 6-311++G(3df,3pd) basis set.

In Table 13, each of the density functionals is used to calculate the enthalpy of formation of $CH_3OOOOCH_3$ using the isodesmic work reactions of Scheme 1. Also included in Table 13 are the average enthalpy and average error for each method across each of the isodesmic reactions. The work reaction results are basis set consistent, with considerable improvements obtained by moving from the double-ζ to the triple-ζ basis set. Only the VSXC and X3LYP methods do not provide an average

TABLE 13: Enthalpy of Formation of $CH_3OOOOCH_3$ from Isodesmic Work Reactions, Using 10 DFT Methods with the 6-31G(d) and 6-311++G(3df,3pd) Basis Sets

		$\Delta_f H°_{298}$						mean absolute
		1-1	1-2	1-3	1-4	1-5	average	error
B3LYP	6-31G(d)	−1.1	−4.1	0.7	0.2	−4.3	−1.7	8.1
	6-311++G(3df,3pd)	−8.1	−8.5	−6.8	−7.9	−8.8	−8.0	1.8
TPSS	6-31G(d)	−4.3	−7.0	−2.3	−3.2	−7.2	−4.8	5.0
	6-311++G(3df,3pd)	−10.7	−10.7	−8.7	−9.8	−11.4	−10.2	0.8
PBE0	6-31G(d)	−1.4	−4.8	0.2	−0.4	−4.9	−2.2	7.6
	6-311++G(3df,3pd)	−8.8	−10.6	−7.8	−8.8	−9.9	−9.2	0.9
O3LYP	6-31G(d)	−2.6	−5.7	−0.1	−1.1	−6.1	−3.1	6.7
	6-311++G(3df,3pd)	−9.6	−10.4	−7.9	−8.9	−11.4	−9.7	0.9
BMK	6-31G(d)	−0.4	−3.9	0.5	0.2	−3.9	−1.5	8.3
	6-311++G(3df,3pd)	−7.6	−8.4	−7.1	−7.5	−8.7	−7.8	2.0
B98	6-31G(d)	−0.7	−4.1	1.1	0.3	−4.2	−1.5	8.3
	6-311++G(3df,3pd)	−8.1	−8.8	−7.1	−7.6	−9.2	−8.2	1.6
B1B95	6-31G(d)	−0.5	−4.0	1.1	0.5	−4.1	−1.4	8.4
	6-311++G(3df,3pd)	−8.0	−8.8	−7.0	−8.2	−9.1	−8.2	1.6
VSXC	6-31G(d)	−18.7	−20.5	−20.4	−19.4	−18.4	−19.5	9.7
	6-311++G(3df,3pd)	−26.4	−25.0	−28.1	−27.2	−23.4	−26.0	16.2
TPSSh	6-31G(d)	−2.1	−5.2	−0.2	−1.1	−5.3	−2.8	7.0
	6-311++G(3df,3pd)	−8.9	−9.4	−7.5	−9.0	−10.0	−9.0	0.9
X3LYP	6-31G(d)	−1.1	−4.1	0.6	0.2	−4.2	−1.7	8.1
	6-311++G(3df,3pd)	−8.2	−8.5	−7.0	−8.0	−4.2	−7.2	2.6

[a] All values are given in kcal mol^{-1}.

TABLE 14: Bond Dissociation Energies for the C−O and O−O Bonds in $CH_3OOOOCH_3$, Calculated Using 10 DFT Methods with the 6-31G(d) and 6-311++G(3df,3pd) Basis Sets[a]

		$CH_3-OOOOCH_3$		$CH_3O-OOOCH_3$		$CH_3OO-OOCH_3$		mean absolute
		BDE	error	BDE	error	BDE	error	error
B3LYP	6-31G(d)	44.2	1.8	16.0	4.0	11.4	2.5	2.8
	6-311++G(3df,3pd)	42.7	3.3	16.3	3.7	11.5	2.4	3.1
TPSS	6-31G(d)	49.1	3.1	11.5	8.5	12.4	1.5	4.4
	6-311++G(3df,3pd)	49.4	3.4	11.7	8.3	12.4	1.5	4.4
PBE0	6-31G(d)	43.1	2.9	16.8	3.2	11.2	2.7	2.9
	6-311++G(3df,3pd)	42.6	3.4	17.6	2.4	12.0	1.9	2.6
O3LYP	6-31G(d)	38.5	7.5	10.4	9.6	8.0	5.9	7.7
	6-311++G(3df,3pd)	37.0	9.0	11.1	8.9	8.2	5.7	7.9
BMK	6-31G(d)	44.6	1.4	19.5	0.5	10.3	3.6	1.8
	6-311++G(3df,3pd)	54.8	8.8	20.5	0.5	11.2	2.7	4.0
B98	6-31G(d)	43.7	2.3	15.8	4.2	10.4	3.5	3.3
	6-311++G(3df,3pd)	42.8	3.2	16.6	3.4	10.8	3.1	3.2
B1B95	6-31G(d)	41.2	4.8	14.9	5.1	8.8	5.1	5.0
	6-311++G(3df,3pd)	40.8	5.2	15.6	4.4	9.3	4.6	4.7
VSXC	6-31G(d)	42.3	3.7	16.1	3.9	23.2	9.3	5.6
	6-311++G(3df,3pd)	40.4	5.6	16.2	3.8	23.0	9.1	6.2
TPSSh	6-31G(d)	47.1	1.1	15.2	4.8	12.7	1.2	2.4
	6-311++G(3df,3pd)	45.8	0.2	16.2	3.8	13.1	0.8	1.6
X3LYP	6-31G(d)	44.2	1.8	16.7	3.3	11.7	2.2	2.4
	6-311++G(3df,3pd)	43.3	2.7	17.2	2.8	11.8	2.1	2.5

[a] All values are given in kcal mol^{-1}.

error below the 2 kcal mol^{-1} threshold, using the triple-ζ 6-311++G(3df,3pd) basis set. These results highlight the significant gains in accuracy that can be obtained when using isodesmic work reactions in conjunction with density functional theory methods.

Finally, we use the DFT data to determine each of the C−O and O−O bond energies in $CH_3OOOOCH_3$ using bond dissociation work reactions. The results are listed in Table 14, and again we do not find the results to be basis set consistent, in that no noticeable gains are made by using the larger basis set. With the 6-311++G(3df,3pd) basis set, the most accurate methods prove to be TPSSh, X3LYP, and PBE0, while with the 6-31G(d) basis set the BMK, TPSSh, X3LYP, B3LYP, and PBE0 methods are the most successful.

Summarizing the DFT results, we find that the density functionals that are suited to studying reaction kinetics generally

prove successful at describing the thermodynamics of $CH_3OOOOCH_3$ and its radicals. Specifically, the hybrid meta-GGA TPSSh was the most accurate functional across all of the calculations, while BMK and B1B95 also performed well. Additionally, the improvements that can be made by using isodesmic work reactions are clearly demonstrated.

Conclusions

Thermochemical properties have been calculated for $CH_3OOOOCH_3$ and its radicals corresponding to C−O and O−O bond cleavage, using high-accuracy composite theoretical methods in conjunction with bond isodesmic work reactions. The enthalpy of formation of $CH_3OOOOCH_3$ is calculated to be −9.8 kcal mol^{-1}, and from this value we suggest a new group additivity enthalpy value of 9.6 kcal mol^{-1} for the O/O_2 group. The bond dissociation energies of $CH_3-OOOOCH_3$, $CH_3O-OOOCH_3$, and $CH_3OO-OOCH_3$ are calculated to be 46.0, 20.0, and 13.9 kcal mol^{-1}. A wide range of DFT methods is tested against our calculated thermochemical parameters, with the most successful methods being TPSSh, B1B95, and B98. Dramatic improvements were made by using isodesmic work reactions, where nearly all of the tested DFT methods reproduced the enthalpy of formation of $CH_3OOOOCH_3$ to within the uncertainty of the reference value.

Acknowledgment. We acknowledge financial support from the ExxonMobil Educational Fund and the New Jersey Institute of Technology Ada C. Fritts Chair. This work was presented in part at the 34th Northeast Regional Meeting of the American Chemical Society (2006).

Supporting Information Available: Geometries (Cartesian coordinates) and enthalpies (hartrees) for $CH_3OOOOCH_3$ and its radicals, internal rotor potentials in the CH_3OOOO, CH_3OOO, and CH_3OO radicals, and spin operator (S^2) values in the CH_3O_x radicals from DFT calculations. This material is available free of charge via the Internet at http://pubs.acs.org.

References and Notes

(1) Tyndall, G. S.; Cox, R. A.; Granier, C.; Lesclaux, R.; Moortgat, G. K.; Pilling, M. J.; Ravishankara, A. R.; Wallington, T. J. *J. Geophys. Res. D* **2001**, *106*, 12157.

(2) (a) Cox, R. A.; Tyndall, G. S. *Chem. Phys. Lett.* **1979**, *65*, 357. (b) Hochanadel, C. J.; Ghormley, J. A.; Boyle, J. W. *J. Phys. Chem.* **1977**, *81*, 3. (c) Horie, O.; Crowley, J. N.; Moortgat, G. K. *J. Phys. Chem.* **1990**, *94*, 8198. (d) Jenkin, M. E.; Cox, R. A. *J. Phys. Chem.* **1991**, *95*, 3229. (e) Kan, C. S.; Calvert, J. G.; Shaw, J. H. *J. Phys. Chem.* **1980**, *84*, 3411. (f) Lightfoot, P. D.; Lesclaux, R.; Veyret, B. *J. Phys. Chem.* **1990**, *94*, 700. (g) Niki, H.; Maker, P. D.; Savage, C. M.; Breltenbach, *J. Phys. Chem.* **1981**, *85*, 877. (h) Sander, S. P.; Watson, R. T. *J. Phys. Chem.* **1981**, *85*, 2960. Sander, S. P.; Watson, R. T. *J. Phys. Chem.* **1980**, *84*, 1664. (i) Tyndall, G. S.; Wallington, T. J.; Ball, J. C. *J. Phys. Chem. A* **1998**, *102*, 2547. (j) Weaver, J.; Meagher, J.; Shortridge, R.; Heicklen, J. **1975**, *4*, 341.

(3) Atkinson, R.; Baulch, D. L.; Cox, R. A.; Crowley, J. N.; Hampson, R. F.; Hynes, R. G.; Jenkin, M. E.; Rossi, M. J.; Troe, J. *Atmos. Chem. Phys. Discuss.* **2005**, *5*, 6295.

(4) (a) Bohr, F.; Henon, E.; García, I.; Castro, M. *Int. J. Quantum Chem.* **1999**, *75*, 671. (b) Ghigo, G.; Maranzana, A.; Tonachini, G. *J. Chem. Phys.* **2003**, *118*, 10575. (c) Henon, E.; Bohr, F.; Chakir, A.; Brion, J. *Chem. Phys. Lett.* **1997**, *264*, 557. (d) Jalbout, A. F.; Zhou, Z.; Li, X. H.; Shi, Y.; Kosmas, A. *Chem. Phys. Lett.* **2006**, *420*, 215. (e) Zhu, R.; Lin, M. C. *PhysChemComm* **2001**, *23*, 1.

(5) (a) Feria, L.; Gonzalez, C.; Castro, M. *Int. J. Quantum Chem.* **2004**, *96*, 380. (b) Hou, H.; Li, J.; Song, X.; Wang, B. *J. Phys. Chem. A* **2005**, *109*, 11206. (c) Hasson, A. S.; Kuwata, K. T.; Arroyo, M. C.; Petersen, E. B. *J. Photochem. Photobiol., A* **2005**, *176*, 218.

(6) (a) Khachatryan, L. A.; Niazyan, O. M.; Mantashyan, A. A.; Vedeneev, V. I.; Tietel'boim, M. A. *Int. J. Chem. Kinet.* **1982**, *14*, 1231. (b) Miller, J. A.; Pilling, M. J.; Troe, J. *Proc. Combust. Inst.* **2005**, *30*, 43.

(7) da Silva, G.; Sebbar, N.; Bozzelli, J. W.; Bockhorn, H. *ChemPhysChem* **2006**, *7*, 1119.

(8) da Silva, G.; Bozzelli, J. W. *J. Phys. Chem. A* **2006**, *110*, 13058.

(9) da Silva, G.; Kim, C.-H.; Bozzelli, J. W. *J. Phys. Chem. A* **2006**, *110*, 7925.

(10) (a) Cool, T. A.; Nakajima, K.; Mostefaoui, T. A.; Qi, F.; McIlroy, A.; Westmoreland, P. R.; Law, M. E.; Poisson, L.; Peterka, D. S.; Ahmed, M., *J. Chem. Phys.* **2003**, *119*, 8356. (b) Taatjes, C. A.; Hansen, N.; McIlroy, A.; Miller, J. A.; Senosiain, J. P.; Klippenstein, S. J.; Qi, F.; Sheng, L.; Zhang, Y.; Cool, T. A.; Wang, J.; Westmoreland, P. R.; Law, M. E.; Kasper, T.; Kohse-Höinghaus, K., *Science* **2005**, *308*, 1887. (c) Taatjes, C. A.; Hansen, N.; Miller, J. A.; Cool, T. A., Wang, J.; Westmoreland, P. R.; Law, M. E.; Kasper, T.; Kohse-Höinghaus, K. *J. Phys. Chem. A* **2006**, *110*, 3254.

(11) Taylor, P. H.; Yamada, T.; Marshall, P. *Int. J. Chem. Kinet.* **2006**, *38*, 489.

(12) Lee, J.; Bozzelli, J. W. *Int. J. Chem. Kinet.* **2003**, *35*, 20.

(13) Senosiain, J. P.; Klippenstein, S. J.; Miller, J. A. *J. Phys. Chem. A* **2006**, *110*, 6960.

(14) Miller, J. H.; McCunn, L. R.; Krisch, M. J.; Butler, L. J. *J. Chem. Phys.* **2004**, *121*, 1830.

(15) Benson, S. W. *J. Am. Chem. Soc.* **1964**, *86*, 3922.

(16) Nangia, P. S.; Benson, S. W. *J. Phys. Chem.* **1979**, *83*, 1138.

(17) Lay, T. H.; Bozzelli, J. W. *J. Phys. Chem. A* **1997**, *101*, 9505.

(18) Cohen, N.; Benson, S. W. *Chem. Rev.* **1993**, *93*, 2419.

(19) Francisco, J. S.; Williams, I. H. *Int. J. Chem. Kinet.* **1988**, *20*, 455.

(20) Kokorev, V. N.; Vyshinskii, N. N.; Maslennikov, V. P.; Abronin, I. A.; Zhidomirov, G. M.; Aleksandrov, Y. A. *Zh. Strukt. Khim.* **1981**, *22*, 9.

(21) (a) Mansergas, A.; Anglada, J. M. *ChemPhysChem* **2007**, *8*, 1534. (b) Mansergas, A.; Anglada, J. M. *J. Phys. Chem. A* **2007**, *111*, 976. (c) Mansergas, A.; Anglada, J. M. *ChemPhysChem* **2006**, *7*, 1488.

(22) Yang, L.-C.; Fang, D.-C. *J. Mol. Struct. (THEOCHEM)* **2004**, *671*, 141.

(23) de Souza Sombrio, P.; Ceolin de Bona, J.; Resende, S. M. *Chem. Phys. Lett.* **2004**, *397*, 144.

(24) Sheng, C. Ph.D. Dissertation, New Jersey Institute of Technology, 2002.

(25) (a) Lay, T. H.; Krasnoperov, L. N.; Venanzi, C. A.; Bozzelli, J. W. *J. Phys. Chem.* **1996**, *100*, 8240. (b) Yamada, T.; Lay, T. H.; Bozzelli, J. W. *J. Phys. Chem. A* **1998**, *102*, 7286.

(26) Ayala, P. Y.; Schlegel, J. *J. Chem. Phys.* **1998**, *108*, 2314 and references therein.

(27) Baboul, A. G.; Curtiss, L. A.; Redfern, P. C.; Raghavachari, K. *J. Chem. Phys.* **1999**, *110*, 7650.

(28) Ochterski, J. W.; Petersson, G. A.; Montgomery, J. A. *J. Chem. Phys.* **1996**, *104*, 2598.

(29) Raghavachari, K.; Stefanov, B. B; Curtiss, L. A. *J. Chem. Phys.* **1997**, *106*, 6764.

(30) Chase, M. W., Jr. *J. Phys. Chem. Ref. Data* **1998**, (Monograph 9), 1.

(31) Cox, J. D.; Wagman, D. D.; Medvedev, V. A. *CODATA Key Values for Thermodynamics*; Hemisphere Publishing: New York, 1984.

(32) Ruscic, B.; Pinzon, R. E.; Morton, M. L.; Srinivasan, N. K.; Su, M.-C.; Sutherland, J. W.; Michael, J. V. *J. Phys. Chem. A* **2006**, *110*, 6592.

(33) Prosen, E. J.; Rossini, F. D. *J. Res. Natl. Bur. Stand.* **1945**, 263.

(34) Pittam, D. A.; Pilcher, G. *J. Chem. Soc., Faraday Trans. 1* **1972**, *68*, 2224.

(35) Hine, J.; Arata, K. *Bull. Chem. Soc. Jpn.* **1976**, *49*, 3089.

(36) Blanksby, S. J.; Ellison, G. B. *Acc. Chem. Res.* **2003**, *36*, 255.

(37) Green, J. H. S. *Chem. Ind.* **1960**, 1215.

(38) Pilcher, G.; Pell, A. S.; Coleman, D. J. *Trans. Faraday Soc.* **1964**, *60*, 499.

(39) Baker, G.; Littlefair, J. H.; Shaw, R.; Thynne, J. C. J. *J. Chem. Soc.* **1965**, 6970.

(40) Khursan, S. L.; Martem'yanov, V. S. *Russ. J. Phys. Chem.* **1991**, *65*, 321.

(41) Frisch, M. J.; Trucks, G. W.; Schlegel, H. B.; Scuseria, G. E.; Robb, M. A.; Cheeseman, J. R.; Montgomery, J. A., Jr.; Vreven, T.; Kudin, K. N.; Burant, J. C.; Millam, J. M.; Iyengar, S. S.; Tomasi, J.; Barone, V.; Mennucci, B.; Cossi, M.; Scalmani, G.; Rega, N.; Petersson, G. A.; Nakatsuji, H.; Hada, M.; Ehara, M.; Toyota, K.; Fukuda, R.; Hasegawa, J.; Ishida, M.; Nakajima, T.; Honda, Y.; Kitao, O.; Nakai, H.; Klene, M.; Li, X.; Knox, J. E.; Hratchian, H. P.; Cross, J. B.; Adamo, C.; Jaramillo, J.; Gomperts, R.; Stratmann, R. E.; Yazyev, O.; Austin, A. J.; Cammi, R.; Pomelli, C.; Ochterski, J. W.; Ayala, P. Y.; Morokuma, K.; Voth, G. A.; Salvador, P.; Dannenberg, J. J.; Zakrzewski, V. G.; Dapprich, S.; Daniels, A. D.; Strain, M. C.; Farkas, O.; Malick, D. K.; Rabuck, A. D.; Raghavachari, K.; Foresman, J. B.; Ortiz, J. V.; Cui, Q.; Baboul, A. G.; Clifford, S.; Cioslowski, J.; Stefanov, B. B.; Liu, G.; Liashenko, A.; Piskorz, P.; Komaromi, I.; Martin, R. L.; Fox, D. J.; Keith, T.; Al-Laham, M. A.; Peng, C. Y.; Nanayakkara, A.; Challacombe, M.; Gill, P. M. W.; Johnson,

B.; Chen, W.; Wong, M. W.; Gonzalez, C.; Pople, J. A. *Gaussian 03*, revision D.01; Gaussian, Inc.: Wallingford, CT, 2003.

(42) (a) Becke, A. D. *Phys. Rev. A* **1988**, *38*, 3098. (b) Lee, C.; Yang, W.; Parr, R. G. *Phys. Rev. B* **1988**, *37*, 785.

(43) Tao, J.; Perdew, J. P.; Staroverov, V. N.; Scuseria, G. E. *Phys. Rev. Lett.* **2003**, *91*, 146401.

(44) Adamo, C.; Barone, V. *J. Chem. Phys.* **1999**, *110*, 6158.

(45) (a) Handy, N. C.; Cohen, A. J. *Mol. Phys.* **2001**, *99*, 403. (b) Handy, N. C.; Cohen, A. J. *Mol. Phys.* **2001**, *99*, 607.

(46) Boese, A. D.; Martin, J. M. L. *J. Chem. Phys.* **2004**, *121*, 3405.

(47) Schmider, H. L.; Becke, A. D. *J. Chem. Phys.* **1998**, *108*, 9624.

(48) Becke, A. D. *J. Chem. Phys.* **1996**, *104*, 1040.

(49) Van, Voorhis, T.; Scuseria, G. E. *J. Chem. Phys.* **1998**, *109*, 400.

(50) Staroverov, V. N.; Scuseria, G. E.; Tao, J.; Perdew, J. P. *J. Chem. Phys.* **2003**, *119*, 12129.

(51) Xu, X.; Goddard, W. A. *Proc. Natl. Acad. Sci. U.S.A.* **2004**, *101*, 2673.

(52) For example, see: (a) Carpenter, J. E.; Weinhold, F. *J. Phys. Chem.* **1988**, *92*, 4295. (b) Carpenter, J. E.; Weinhold, F. *J. Phys. Chem.* **1988**, *92*, 4306.

(53) Truhlar, D. G. *J. Comput. Chem.* **1991**, *12*, 266.

(54) Pitzer, K. S.; Gwinn, W. D. *J. Chem. Phys.* **1942**, *10*, 428.

(55) (a) Matthews, J.; Sinha, A.; Francisco, J. S. *J. Chem. Phys.* **2005**, *122*, 221101. (b) Sheng, C. Y.; Bozzelli, J. W.; Dean, A. M.; Chang, A. Y. *J. Phys. Chem. A* **2002**, *106*, 7276. (c) Sumathi, R.; Green, W. H. *Phys. Chem. Chem. Phys.* **2003**, *5*, 3402.

(56) Benson, S. *Thermochemical Kinetics*, 2nd ed.; Wiley-Interscience: New York, 1976.

(57) Lay, T. H. Ph.D. Dissertation, New Jersey Institute of Technology, 1994.

(58) Dybala-Defratyka, A.; Paneth, P.; Pu, J.; Truhlar, D. G. *J. Phys. Chem. A* **2004**, *108*, 2475.

(59) Zhao, Y.; Truhlar, D. G. *J. Chem. Theory Comput.* **2005**, *1*, 415.

(60) Zhao, Y.; Pu, J.; Lynch, B. J.; Truhlar, D. G. *Phys. Chem. Chem. Phys.* **2004**, *6*, 673.